JOURNAL OF THE AMERICAN WATER RESOURCES ASSOCIATION
FEBRUARY AMERICAN WATER RESOURCES ASSOCIATION 2006

INFLUENCE OF TWO WOODY RIPARIAN SPECIES ON CRITICAL CONDITIONS FOR STREAMBANK STABILITY: UPPER TRUCKEE RIVER, CALIFORNIA[1]

Andrew Simon, Natasha Pollen, and Eddy Langendoen[2]

ABSTRACT: Over the past 35 years, a trend of decreasing water clarity has been documented in Lake Tahoe, attributable in part to the delivery of fine grained sediment emanating from upland and channel erosion. A recent study showed that the Upper Truckee River is the single largest contributor of sediment to Lake Tahoe, with a large proportion of the sediment load emanating from streambanks. This study combines field data with numerical modeling to identify the critical conditions for bank stability along an unstable reach of the Upper Truckee River, California. Bank failures occur during winter and spring months, brought on by repeated basal melting of snow packs and rain-on-snow events. Field studies of young lodgepole pines and Lemmon's willow were used to quantify the mechanical, hydrologic, and net effects of riparian vegetation on streambank stability. Lemmon's willow provided an order of magnitude more root reinforcement (5.5 kPa) than the lodgepole pines (0.5 kPa); the hydrologic effects of the species varied spatially and temporally and generally were of a smaller magnitude than the mechanical effects. Overall, Lemmon's willow provided a significant increase in bank strength, reducing the frequency of bank failures and delivery of fine grained sediment to the study reach of the Upper Truckee River.
(KEY TERMS: infiltration; riparian vegetation; rivers/streams; streambank stability; erosion; root reinforcement.)

Simon, Andrew, Natasha Pollen, and Eddy Langendoen, 2006. Influence of Two Woody Riparian Species on Critical Conditions for Streambank Stability: Upper Truckee River, California. Journal of the American Water Resources Association (JAWRA) 42(1):99-113.

INTRODUCTION

The Lake Tahoe Basin has a history of human influence and exploitation dating back to the 1850s. Activities such as logging, road construction, mining, overgrazing, and urbanization have led to degradation of land and water resources and threaten irreparable damage to the lake. In particular are concerns over lake clarity that have been partly attributed to the delivery of fine grained sediment emanating from upland and channel erosion. Over the past 35 years a trend of decreasing water clarity, as measured by secchi depth, has been documented (Jassby *et al.,* 1999, 2003).

A number of studies have been completed in the past 25 years to address sediment delivery issues from various watersheds in the Lake Tahoe Basin. Most of these studies have focused on only a few streams within the watershed (Kroll, 1976; Glancy, 1988; Hill and Nolan, 1990; Nolan and Hill, 1991; Stubblefield, 2002). Results of these studies indicate that channels and particularly channel banks may be an important source of fine grained sediment. Recent work by Reuter and Miller (2000) and Rowe *et al.* (2002) used suspended sediment transport data from the Lake Tahoe Monitoring Program (LTMP), which brought together data from streams throughout the watershed. Most of the sediment is delivered during the spring snowmelt period (predominantly May and June), which correlates well with the springtime reduction in secchi depth. Because lake clarity is related to the very fine particles that remain in suspension for a long time, it is essential to identify the volume and sources of fine grained materials.

A recent study by the U.S. Department of Agriculture-Agricultural Research Service's (USDA-ARS) National Sedimentation Laboratory (Simon *et al.,* 2003) combined geomorphic evaluations of about 300 sites with numerical modeling of selected watersheds and detailed analysis of all available suspended sediment data to provide a comprehensive evaluation of

[1]Paper No. 04204 of the *Journal of the American Water Resources Association* (JAWRA) (Copyright © 2006). **Discussions are open until August 1, 2006.**

[2]Respectively, Research Geologist, Geologist, and Research Hydaulic Engineer, USDA-ARS National Sedimentation Laboratory, 598 McElroy Drive, P.O. Box 11578, Oxford, Mississippi 38655 (E-Mail/Pollen: npollen@msa-oxford.ars.usda.gov).

the state of knowledge on the delivery of suspended sediment to Lake Tahoe. Undisturbed channels tend to have greater proportions of their sediment load emanating from upland areas. For example, in the General Creek watershed (Figure 1), numerical modeling shows that about 78 percent of the fine grained materials passing the gage farthest downstream originate from upland sources. Conversely, disturbed channels have a greater proportion of their sediment load emanating from streambanks. Ward Creek supplies almost five times the amount of fine grained material from streambanks that General Creek supplies. Blackwood Creek provides about 217 $m^3/y/km$, about 14 times the amount of streambank derived sediment per kilometer of channel than from General Creek, almost four times more than Ward Creek, but 66 percent less than from the Upper Truckee River. The Upper Truckee River is the single largest contributor of sediment to Lake Tahoe.

To accurately predict streambank instability and subsequent volume of material delivered to stream channels, a detailed study that accounts for all of the controlling processes and variables was initiated in a rapidly eroding reach of the Upper Truckee River. In addition, detailed analyses of the hydrologic and mechanical effects of existing riparian vegetation on streambank stability were conducted and evaluated as a potential means of enhancing bank strength. Riparian vegetation plays a number of roles in protecting streambanks from erosion by both particle entrainment and mass wasting. However, the positive and negative effects of riparian vegetation on streambank stability are often hard to quantify, largely due to the inherent spatial and temporal variability in root network development and bank properties. As such, a combination of field data collection and modeling is needed to estimate the ways in which riparian vegetation interacts with fluvial and mass wasting processes and affects streambank stability. This paper describes the results of a study on critical conditions for bank stability using the Bank-Stability and Toe Erosion Model of Simon *et al.* (1999, 2000)

PURPOSE AND SCOPE

A detailed study of streambank erosion processes was conducted in the Washoe Meadows reach of the Upper Truckee River (Figure 1). The main purposes

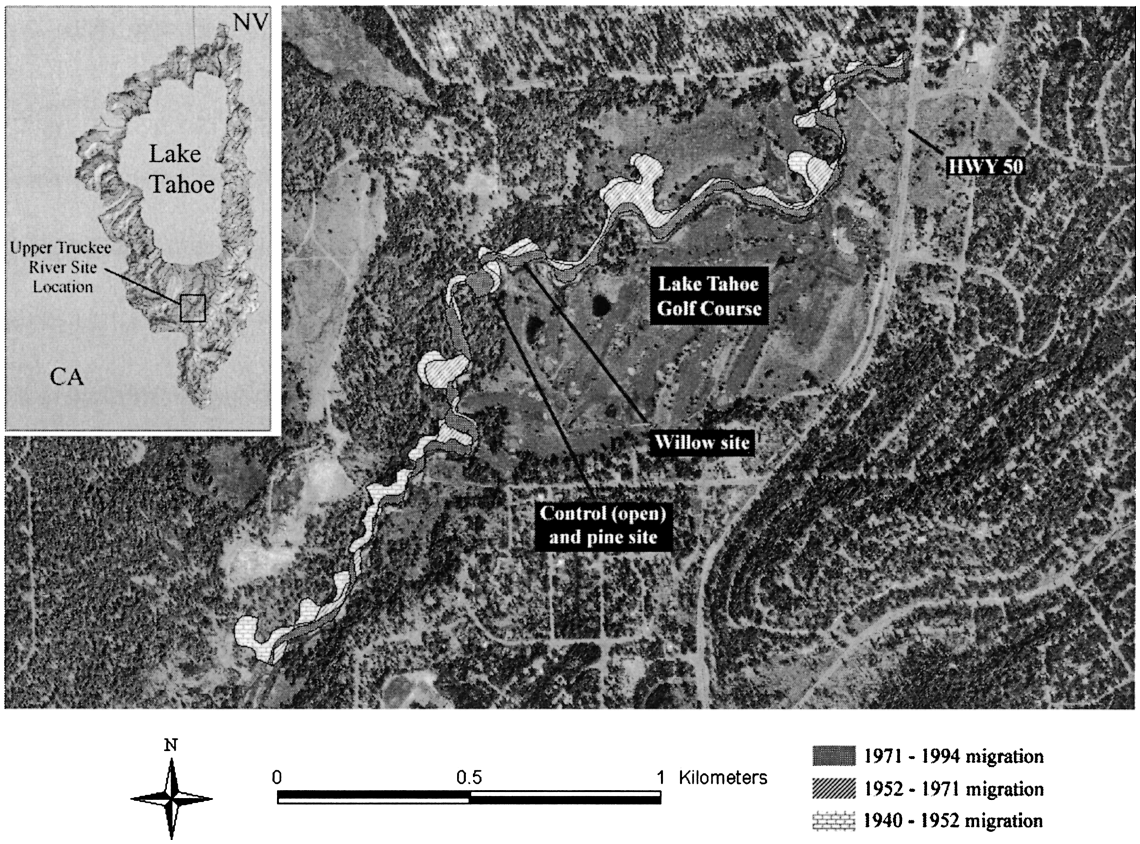

Figure 1. Aerial Photograph and (inset) Location Map of the Washoe Meadows Reach of the Upper Truckee River, California, Showing Migration of the Channel Over Time and the Location of the Two Research Sites.

of this investigation were to quantify the critical conditions for streambank failure, identify the controlling processes, and evaluate the potential use of two common riparian species as a means of reducing the frequency of bank failures. Two sites along actively eroding streambanks were selected for study because of their accessibility and because they represented three typical bank top conditions: bare, with young lodgepole pine, and with young willows. The lodgepole pine and control sites were along the same reach of the stream, with a total bank length for this reach of approximately 60 m, compared to a reach length of approximately 30 m for the willow site slightly downstream (Figure 1a). The sites have been monitored from August 2003 onward, including data from August 2003 to April 2004 in this study.

Quantifying Streambank Stability

Conceptual models of bank retreat and the delivery of bank sediments to the flow emphasize the importance of interactions between hydraulic forces acting at the bed and bank toe and gravitational forces acting on *in situ* bank materials (Carson and Kirkby, 1972; Thorne, 1982; Simon *et al.,* 1991; Langendoen, 2000). Failure occurs when erosion of the bank toe and the channel bed adjacent to the bank increase the height and angle of the bank to the point that gravitational forces exceed the shear strength of the bank material. After failure, failed bank materials may be delivered directly to the flow and deposited as bed material, dispersed as wash load, or deposited along the toe of the bank as intact blocks or as smaller, dispersed aggregates (Simon *et al.,* 1991).

Hydraulic Forces and Resistance: Calculating Hydraulic Erosion. A submerged jet test device is used to estimate the resistance of materials to hydraulic forces in fine grained materials *in situ* (Hanson, 1990, 1991; Hanson and Simon, 2001). The device shoots a jet of water at a known pressure head onto the streambed, causing it to erode at a given rate. As the bed erodes, the distance between the jet and the bed increases, resulting in a decrease in applied shear stress. Theoretically, the rate of erosion beneath the jet decreases asymptotically with time to zero. A critical shear stress for the material can then be calculated from the field data as that shear stress where there is no erosion.

The rate of scour ε (m/s) is assumed to be proportional to the shear stress in excess of a critical shear stress and is expressed as

$$\varepsilon = k\,(\tau_o - \tau_c)^a \qquad (1a)$$

where k is the erodibility coefficient (m^3/N-s), τ_o is the average boundary shear stress (Pa), τ_c is the critical shear stress (Pa), and a is an exponent assumed to equal 1.0. The quantity (τ_o - τ_c) is the excess shear stress (Pa).

Average boundary shear stress, representing the stress applied by flowing water along the edge of the bank, is calculated from channel geometry and stage data collected at the sites as

$$\tau_o = \gamma\, R\, S \qquad (1b)$$

where γ is the unit weight of water (N/m^3), R is the hydraulic radius (m), and S is the channel gradient (m/m). An inverse relation between τ_c and k occurs when soils exhibiting a low tc have a high k or when soils having a high τ_c have a low k.

The measure of material resistance to hydraulic stresses is a function of both τ_c and k. Based on observations from across the United States, k can be estimated as a function of τ_c (Hanson and Simon, 2001). This is generalized to

$$k = 0.1\,\tau_c^{-0.5} \qquad (2)$$

Two jet tests were conducted at each site where cohesive bed or bank toe material was present. The τ_c values and k values for cohesive materials in this study were obtained by direct measurement with the jet test device. Results are summarized in Table 1. Erosion of bank toe materials can then be calculated using Equations (1a) and (1b). For coarse grained materials, bulk samples were obtained for particle size analysis. Critical shear stress of these types of materials can then be calculated using conventional (Shields type) techniques as a function of particle size and weight.

The magnitude of bank toe erosion and bank steepening by hydraulic forces is calculated using a bank toe erosion algorithm incorporated into the Bank Stability Model (BSM) (Simon *et al.,* 1999). The algorithm calculates the hydraulic forces acting on the bank face for a particular flow event. Flows are discretized as simple, rectangular hydrographs with the user specifying flow depth, channel gradient, and duration of the flow. The boundary shear stress exerted by the flow on each node is determined by dividing the flow area at a cross section into segments that are affected only by the roughness on the bank or on the bed and then further subdividing to determine the flow area affected by the roughness on each node. The line dividing the bed affected and bank affected segments is assumed to bisect the average bank angle and the average bank toe angle. The hydraulic radius of the flow on this segment is the area of the segment (A) divided by the wetted perimeter of the segment

TABLE 1. Geotechnical Parameters Obtained From Borehole Shear Tests and Submerged Jet Testing at Sites Along the Upper Truckee River.

Bank Layer	Layer Thickness (m)	c´ (kPa)	ϕ´ (degrees)	τ_c (Pa)	k (cm^3/N-s)
1	0.3	0.6	31	0.09	0.335
2	0.7	0.6	26	0.09	0.335
3	0.6	1.3	26	0.71	0.118
4	0.7	2.9	29	19.44	0.023
5	0.4	0.1	32	5.00	0.045
Bank Toe	–	–	–	1.05	3.770

(P_n), and S is the channel slope. Fluid shear stresses along the dividing lines are neglected when determining the wetted perimeter. An average erosion distance is computed by comparing the boundary shear stress with critical shear stress and erodabilty for each node for the specified duration of the peak.

Geotechnical Forces and Resistance: Calculating Mass-Bank Stability. Bank stability was analyzed using the limit equilibrium method, based on static equilibrium of forces and/or moments (Bishop, 1955). Streambank failure occurs when gravitational forces that tend to move soil downslope exceed those forces that resist movement (driving forces exceed resisting forces). The potential for failure is usually expressed by a factor of safety (F_S), defined as the ratio of resisting to driving forces or moments. The BSM performs stability analysis of planar slip failures and accounts for the important driving and resisting forces that control bank stability. Bank geometry, soil shear strength (effective cohesion, $c´$, and angle of internal friction, $\phi´$), pore water pressure, confining pressure, and mechanical and hydrologic effects of riparian vegetation are used to numerically determine the critical conditions for bank stability.

To properly determine the resistance of bank materials to erosion by mass movement, data must be acquired for those characteristics that control shear strength, that is, cohesion, angle of internal friction, pore water pressure, and bulk unit weight. Cohesion and friction angle data can be obtained from standard laboratory testing (triaxial shear or unconfined compression tests) or by *in-situ* testing with a borehole shear test (BST) device (Lohnes and Handy, 1968; Lutenegger and Hallberg, 1981; Thorne *et al.,* 1981; Little *et al.,* 1982; Simon and Castro, 2003). The BST provides direct, drained shear strength tests on the walls of a borehole. The BST results for the Upper Truckee River sites are summarized in Table 1.

The BSM of Simon *et al.* (1999) was developed for use with multilayered banks with complex geometries. The model accounts for the geotechnical resisting forces by using the failure criterion of the Mohr-Coulomb equation for the saturated part of the failure surface

$$S_r = c´ + (\sigma - \mu) \tan \phi´ \quad (3a)$$

where μ is the pore pressure (kPa) and $\phi´$ is the angle of internal friction (degrees). For the unsaturated part of the failure surface the criterion as modified by Fredlund *et al.* (1978) is used,

$$S_r = c´ + (\sigma - \mu_a) \tan \phi´ + (\mu_a - \mu_w) \tan \phi^b \quad (3b)$$

where S_r is the shear strength (kPa), $c´$ is the effective cohesion (kPa), σ is the normal stress (kPa), μ_a is the pore air pressure (kPa), μ_w is the pore water pressure (kPa), $(\mu_a - \mu_w)$ is the matric suction or negative pore-water pressure (kPa), and $\tan \phi^b$ is the rate of increase in shear strength with increasing matric suction. The quantity $(\mu_a - \mu_w)\tan \phi^b$ represents the additional strength provided by matric suction along the unsaturated part of the failure plane and is reflected in the apparent or total cohesion (c_a, in kPa) term although this does not signify that matric suction is a true form of cohesion (Fredlund and Rahardjo, 1993)

$$c_a = c´ + (\mu_a - \mu_w) \tan \phi^b \quad (4)$$

The geotechnical driving force is given by the term

$$F = W \sin\beta \quad (5)$$

where F is the driving force acting on bank material (N), W is the weight of failure block (N), and β is the angle of the failure plane (degrees).

Quantifying the Influence of Vegetation on Bank Stability

Riparian vegetation has both mechanical and hydrologic effects on streambank stability, some of which improve bank stability and some of which are destabilizing (Table 2) (Simon and Collison, 2002). The mechanical effects are for the most part beneficial. Roots anchor themselves into the soil to support the above ground component of the plant and in doing so produce a reinforced soil matrix (Greenway, 1987). As soil is strong in compression but weak in tension and, conversely, plant roots are weak in compression but strong in tension, when the two are combined they produce a matrix of reinforced earth that is stronger than the soil or the roots independently (Thorne, 1990). The roots, therefore, provide reinforcement by transferring shear stress in the soil to tensile resistance in the roots (Gray and Sotir, 1996). The disadvantageous mechanical impacts of vegetation on soil stability are associated with the forces exerted from the above ground component of the vegetation. The weight of the vegetation, in particular large, mature trees, produces a surcharge on the slope or streambank, increasing the driving forces acting in the downslope direction, and reducing the soil stability by various degrees, although this effect can be small (Simon and Collison, 2002).

TABLE 2. Stabilizing and Destabilizing Effects of Riparian Vegetation on Streambank Stability.

	Mechanical	Hydrologic
Stabilizing Effects	Increased soil strength due to roots	• Canopy interception • Transpiration
Destabilizing Effects	Surcharge	• Increased infiltration rate and capacity

The beneficial hydrological effects of vegetation on bank stability also include processes that occur above and below ground. Vegetation removes water from the root zone for use in the processes occurring in the above ground biomass (Dingman, 2001). Pore water pressures in the soil hence remain lower, and the likelihood of mass failure is reduced (Selby, 1993). The hydrologic disadvantages of vegetation on bank stability are related to the way in which soil infiltration characteristics are altered both at the soil surface and deeper within the soil profile. At the surface, canopy interception and stem flow tend to concentrate rainfall locally around the stems of plants, creating higher local pore water pressures (Durocher, 1990; Simon and Collison, 2002). The presence of stems and roots at the soil surface can also act to disturb the imbrication of the soil, hence increasing infiltration capacity. An increase in infiltration capacity creates higher pore water pressures inside the streambank, hence reducing its stability.

Quantifying Root Reinforcement. The theory for quantifying root reinforcement stems from literature developed to calculate the increased strength added to other composite materials used in the construction industry, such as reinforced concrete. Greenway (1987) notes that the magnitude of root reinforcement depends on root growth and density, root tensile strengths, root tensile modulus values, root tortuosity, soil root bond strengths, and the orientation of roots to the principal direction of strain. The most common method used to estimate root reinforcement of soils are physically based force equilibrium models, such as the simple perpendicular root model developed by Waldron (1977) and modified by Wu *et al.* (1979). These root reinforcement models are based on the Coulomb equation, Equation (3a), in which soil-shearing resistance is calculated from cohesive and frictional forces. Roots are assumed to extend vertically across a horizontal shearing zone, with roots acting like laterally loaded piles. The increased shear strength due to roots (ΔS) is treated as a simple add-on factor to the soil strength. The ΔS is calculated using the root tensile strengths and the cross sectional area of the roots relative to the area of the shear surface Wu *et al.* (1979),

$$\Delta S = T_r \, (A_R/A) \, 1.2 \tag{6}$$

where T_r is the root tensile strength, A_R/A is the root area ratio (dimensionless), A is the area of the soil (m^2), and A_R is the area of roots (m^2).The value 1.2 was used by Wu *et al.* (1979) to replace the term in Waldron (1977) that accounts for the angle of shear distortion and soil friction angle. Sensitivity analysis carried out by Wu *et al.* (1979) showed that this term was fairly insensitive to changes in soil properties and approximated 1.2 under most conditions.

Several assumptions are made by the Wu *et al.* (1979) model. Investigations by Pollen (2004) and Pollen *et al.* (2004) have shown that the most critical of these assumptions for accurately predicting root reinforcement is the assumption that all of the roots attain ultimate tensile strength simultaneously during soil shearing. In reality, roots break progressively, producing large overestimations in ΔS in the models of Waldron (1977) and Wu *et al.* (1979). A new root reinforcement model (RipRoot) was developed based on fiber bundle theory to account for progressive root breaking during shearing (Pollen *et al.,* 2004). As with

Wu *et al.* (1979), the RipRoot model produces an add-on factor to soil strength representing root reinforcement. Comparison of results using RipRoot compare well with laboratory direct-shear tests of root permeated soils (Pollen *et al.,* 2004).

Quantifying Root Characteristics. Two riparian plant species typical of the Upper Truckee River were selected for testing: lodgepole pine and Lemmon's willow. Root tensile strengths and stress displacements were measured using a "Root Puller" device based on a design by Abernethy (1999). This is composed of a metal frame with a winch attached to a load cell and displacement transducer, both connected to a data logger. The Root Puller was attached to the bank face, and different size roots were attached to the load cell and displacement transducer. Cranking the winch applies a tensile stress to the root (measured as a load, in kg) that increases until tensile failure of the root occurs. The diameter of each root was recorded along with the logged history of tensile load and shear displacement. The maximum load applied to each root before breaking and root diameter were used to calculate the tensile strength of each root. Relations of root diameter and tensile strength were established for each species tested to use as input to the root reinforcement model, RipRoot (Pollen, 2004; Pollen *et al.,* 2004). Fifty roots of each species were tested for tensile strength.

The root systems of lodgepole pine and Lemmon's willow were examined and recorded using the wall profile method of Bohm (1979). In this case, the bank face acted as the profile wall, and visible roots were cut back to the face of the bank so that a grid 1 m by 1 m with 0.1 m increments could be placed against it. Three grids were analyzed for each species. The use of the bank face as the wall profile means that the exposed roots may have been subject to weathering; only those roots that had not been washed away by flow events could be recorded. Root diameters were measured and recorded according to depth in the bank profile. Estimates of ΔS provided by the roots of each species were calculated using the root architecture and tensile strength data that were collected. To obtain an estimate of increased soil strength due to roots, the RipRoot model uses the distribution of root diameters and the corresponding species specific root diameter tensile strength curve.

To investigate the hydrologic effects of the two species, nests of three tensiometers were installed at depths of 0.3 m, 1.0 m, and 1.5 m. The data from these tensiometers provided pore water pressure data in a field situation, allowing for comparison between two vegetative treatments and a control site. The treatments consisted of: an unvegetated "open" plot (control site); a plot of young (two-year to five-year old) lodgepole pine saplings (*Pinus contorta*); and a plot of young (approximately five-year old) Lemmon's willow (*Salix lemmonii*). The banks at each site were nearly vertical, with vegetation growing on top of the banks but not on the bank face. Bank heights along the study reach ranged from approximately 2.5 to 3.0 m. Banks at the control pine site were composed of two layers: from the top of the profile down to approximately 2.5 m the soil was a sandy loam, with gravel content increasing with depth through this layer; below the sand gravel layer the profile was dominated by clay. At the willow site, only the sand and gravel layer was evident.

Root Tensile Strengths. Regressions of the form $y = ax^{-b}$ were fitted to the root diameter tensile strength data (Figure 2). The shape of these curves is consistent with those reported in the literature (Gray and Sotir, 1996; Simon and Collison, 2002), with small roots having greater strength per unit area. It is interesting to note that the strength of individual roots of comparable size from the two species were similar. Any differences in ΔS, therefore, will be a function of the number and distribution of those roots in the bank profile. The r^2 values for the two curves were 0.62 and 0.78 for Lemmon's willow and lodgepole pine, respectively ($p < 0.0001$). The scatter seen in the tensile strength data is consistent with that seen for other species in previous studies (Simon and Collison, 2002; Pollen *et al.,* 2004) and is likely due to a variety of factors including soil moisture, soil texture, and nutrient status.

In addition to variations in root tensile strength with root diameter, variations in root wood strength have even been found to occur along roots with a fairly constant diameter, the degree of variation being related to the root architecture of the plant (Stokes and Mattheck, 1996). It is possible that some of the scatter in the tensile strength data is associated with changes in strength along the length of the roots. During field work, measurements were not made to determine the length along the roots at which the load cell was attached because it was not feasible to establish either the length to the end of the root or the length to the place in the soil matrix where the root branched from another root. It is therefore difficult to know to what extent these variations in tensile strength along the length of the roots may have affected the scatter of the data collected.

Root Size Distributions, Root Area Ratio, and Increase in Cohesion Due to Roots (ΔS). Analysis of root size distribution data showed that the numbers and distribution of roots of different sizes varied considerably between the two species; Lemmon's willow had much greater root density, especially in the

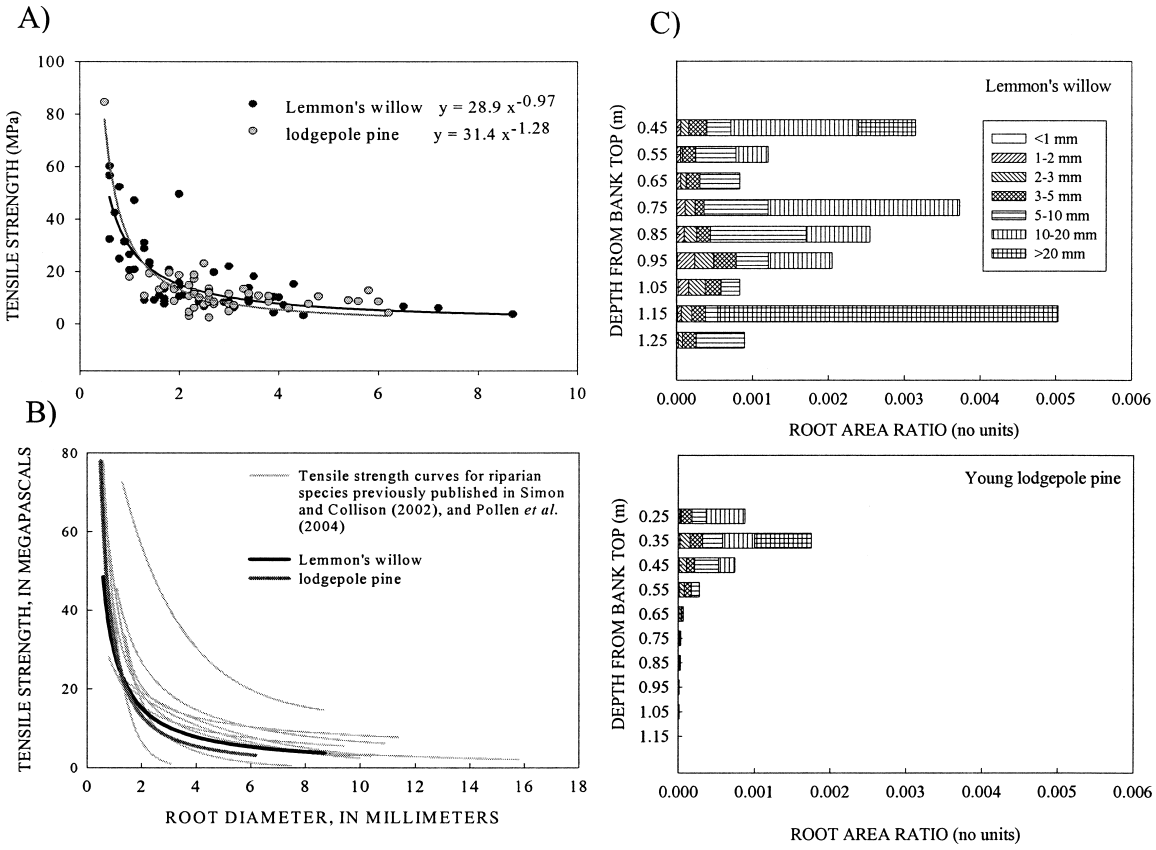

Figure 2. (A) Tensile Strength and Root Diameter Relations for Lemmon's Willow and Lodgepole Pine on the Upper Truckee River, California. (B) Comparison of Two Species Tested in This Study to Other Riparian Species Tested by Simon and Collison (2002) and Pollen *et al.* (2004). (C) Root Area Ratio Measurements by Diameter Size Class for Lemmon's Willow and Lodgepole Pine on the Upper Truckee River, California.

smaller root diameter size classes, between 0.1 and 3 mm. Data for Lemmon's willow showed that roots in the smallest diameter size classes (< 1 mm and 1 to 2 mm) were prevalent within the middle and lower sections of the bank profile; the number of roots of less than 1 mm peaked at a depth of 1.0 m. For the young lodgepole pine trees studied, the number of roots in all diameter size classes decreased with increasing depth in the bank profile, whereas the willow roots were more evenly distributed throughout the whole soil depth studied. For both species, roots 2 mm to 3 mm in diameter were most prevalent throughout the entire profile, making up 36 and 26 percent of the roots measured for the willow and pine, respectively.

Figure 2 shows the contribution made to root area ratio (RAR) by each of the root diameter size classes. Large roots dominated the RARs; despite the large number of smaller roots present, their contribution to overall RAR was small since many hundreds of roots may be required to provide the cross sectional area of a single larger root. The RAR pattern was similar to the patterns observed for root numbers. For willow, RAR remained fairly constant from the surface to the middle of the bank profile studied, then declined with depth. In contrast, lodgepole pine exhibited a steady decline in RAR with increasing depth in the streambank. Following the trend noted in the number of roots counted for each species, the RAR for the Lemmon's willow (0.0023) was much larger than that of lodgepole pine (0.0004); the maximum willow RAR at any depth was more than double the maximum RAR for lodgepole pine. Both values were within the range of RARs calculated previously for other riparian species (Pollen *et al.,* 2004), but the RAR of Lemmon's willow was more than an order of magnitude higher than that of lodgepole pine.

These trends can be explained by considering the way in which lodgepole pine and Lemmon's willow root networks develop. The pines tend to develop a strong taproot from which mainly woody roots branch, particularly from the upper part of the taproot. Although the willow trees also tend to form a deeply anchored taproot, lateral branching from this taproot seemed to be much more uniform with soil depth. In addition, the willow networks possessed many small, fine roots (< 3 mm in diameter) with numerous finer,

fibrous roots also present that were too small to measure. The propagation of Lemmon's willow by sending out lateral runners at various soil depths to form new shoots above ground also helps to explain its more even root distribution.

Although the tensile strength curves of the two species are very similar, differences in root architecture had a large impact on RARs and consequently on resulting values of increased cohesion due to roots (ΔS). The resulting increase in ΔS was 0.5 kPa for lodgepole pines and 5.5 kPa for Lemmon's willow. This is a significant difference given the generally low cohesive strength values associated with soils along the study reach, making Lemmon's willow a good selection for enhancing the strength of the top meter of soil through root reinforcement.

EFFECTS OF VEGETATION ON STREAMBANK HYDROLOGY

To investigate the hydrologic effects of vegetation on pore water pressures and bank strength, general trends of matric suction at the two vegetated sites were compared to values at the control site (Figure 3). The resulting effects on additional soil cohesion through differences in matric suction are shown in Figure 4. The 30 cm tensiometer at the willow site showed less matric suction compared to the control, with resulting cohesion values for Lemmon's willow of 8 to 2 kPa less than the control for the entire monitoring period (Figure 4). This is possibly related to two effects: a canopy that shades the ground surface and considerable soil disturbance from high root density in the upper 30 cm of the bank profile. At a depth of 30 cm at the lodgepole pines plot, matric suction values were greater than the control until mid-November, when the soil became wetter than the control site for the remainder of the monitoring period (approximately 0.5 kPa reduction in cohesion). At the 30 cm, matric suction values for the vegetated sites were more responsive to rainfall/snowmelt than the control because of the presence of root networks that allowed greater infiltration by preferential flow along large roots.

At 100 cm, the vegetated sites were drier than the control throughout the summer due to the removal of soil moisture by evapotranspiration. In addition, the onset of lower matric-suction values at the vegetated plots occurred later than at the control plot at 100 cm depth, reflecting a lag caused by evapotranspiration from the summer months (Figure 3). For both species, the effect of the higher matric-suction values resulted in levels of cohesion 8 to 10 kPa greater than the control until December, when these values decreased rapidly due to periodic melting of snow (Figure 4). It was noted that the soil at 100 cm at the Lemmon's willow site stayed drier longer than the corresponding depth at the pine site, not reaching minimum matric-suction values until mid-January, compared to late December in the case of lodgepole pine (Figure 3). This may be because the willow trees form a much denser stand of vegetation than the individual pine saplings, which are shorter and less dense. This difference in stem density may have affected the depth of snow accumulation at each site during the first few snow events of the winter season. For the remainder of the monitoring period beyond mid-December, both vegetated plots showed a slight positive effect on soil cohesion values at 100 cm depth (Figure 4).

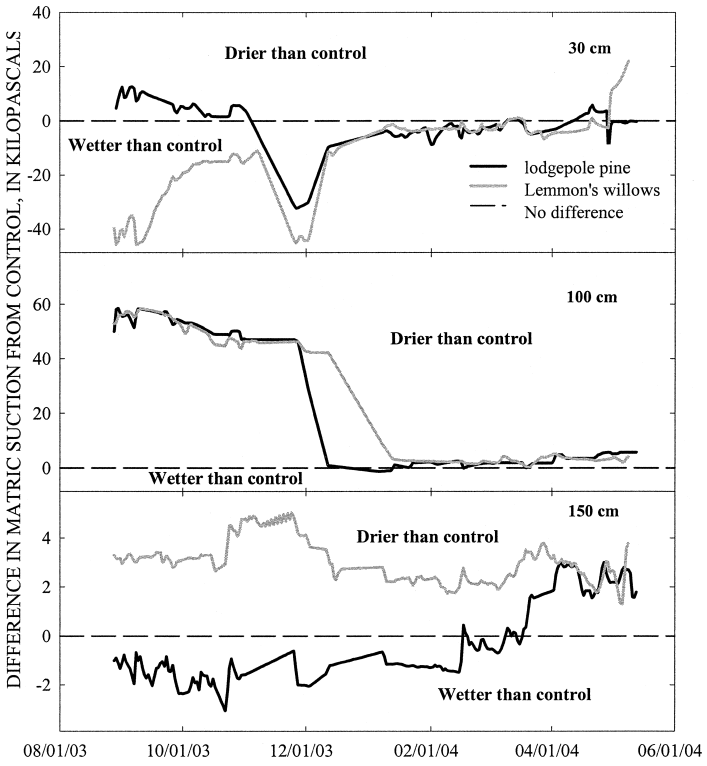

Figure 3. Matric Suction Values for Lodgepole Pine and Lemmon's Willow Relative to the Control.

Matric suction values and resulting changes to streambank cohesion varied little from the control 150 cm below the bank top. For Lemmon's willow there was approximately a 1 kPa increase in cohesion compared to the control; even less benefit was seen at the lodgepole pine site (Figure 4). Vegetation has much less effect at this depth as rooting density declines with increasing depth in the soil profile, decreasing to minimum values below 0.5 m for lodgepole pine and below 1.2 m for Lemmon's willow

(Figure 2). In addition, at this depth matric-suction values are affected more by longer term fluctuations in the local ground water level than water availability at the soil surface.

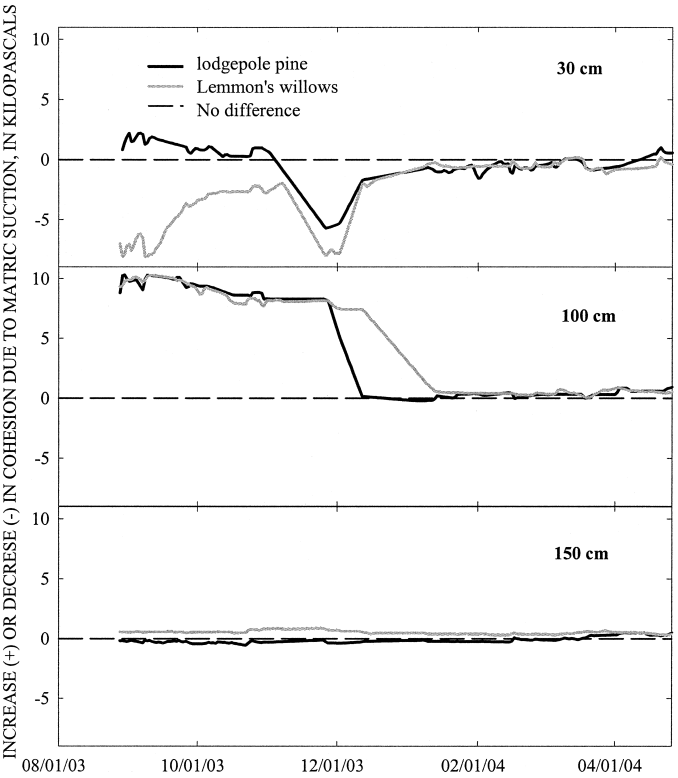

Figure 4. Change in Cohesion Values Due to Matric Suction for Lodgepole Pine and Lemmon's Willow Relative to the Control. Positive values represent increased apparent cohesion (drier soil), and negative values indicate reduced apparent cohesion (wetter soil).

During each of the monitored seasons, additional cohesion from matric suction was greatest at 100 cm, with little benefit from vegetation at the shallowest depths. Variations between species and between seasons were smallest at the 150 cm soil depth. Mean differences in cohesion for each vegetated treatment relative to the control are summarized by season in Table 3. These figures confirm the general trends discussed in the preceding paragraphs. During autumn 2003, the mean amount of cohesion added to the streambanks by the hydrologic effects of riparian vegetation was approximately 9 kPa (Table 3). During the winter and spring seasons, however, this additional cohesion was lost due to preferential flow along roots from basal snowmelt and rain-on-snow events.

Bank Stability Modeling

Tensiometer data and root reinforcement estimates were used in combination with surveyed bank geometry and geotechnical data (Table 1) as inputs for the BSM to assess the critical conditions for bank failure and the relative contributions of the mechanical and hydrologic effects of the two vegetative treatments on streambank stability. Model runs were carried out using a modified form of version 3.4 in which time series tensiometer and stage data can be used to account for hydraulic scour in the toe erosion algorithm and changing flow depths and bank geometries in the bank stability algorithm.

Stage and tensiometer data were split into discrete time periods so that toe erosion and resulting changes in bank geometry could be computed. After each period of toe erosion, bank geometry was updated and the

TABLE 3. Mean Increases in Cohesion Due to Hydrologic Reinforcement at the Two Vegetated Plots.

Season	Treatment	Difference in Matric Suction From Control (kPa)			Associated Increase in Cohesion (kPa)			Weighted Mean Increase in Cohesion (kPa)
		30 cm	100 cm	150 cm	30 cm	100 cm	150 cm	
Autumn 2003	Pines	6.1	53.4	-1.7	1.1	9.4	-0.3	0.89
	Willows	-25.4	52.3	3.3	-4.5	9.2	0.6	0.68
Winter 2003 to 2004	Pines	-8.0	11.2	-0.8	-1.4	2.0	-0.1	0.08
	Willows	-10.5	18.3	3.0	-1.9	3.2	0.5	0.27
Spring 2004	Pines	0.2	4.5	2.3	0.04	0.8	0.4	0.15
	Willows	1.7	3.4	2.6	0.3	0.6	0.5	0.17

Note; Based on matric suction data obtained from the nests of tensiometers installed at the Upper Truckee River sites and compared to the matric suction at the control site.

stability algorithm was run. If at any point during the simulation period the factor of safety (FS) fell below 1.0, the bank was considered to have failed, and again the bank profile was updated before continuing with further FS calculations. In this way, a time series of the FS was constructed for the control and vegetated plots. The original profile and geotechnical parameters from the control site were used as a starting point for each treatment, but the tensiometer data from the vegetated plots were substituted into the respective model runs. To differentiate between the mechanical and hydrologic effects of the vegetation, model runs were repeated for the vegetated plots adding the root reinforcement values (ΔS) for each species.

CRITICAL CONDITIONS FOR BANK FAILURE

Model results showed three predicted failures over the monitoring period, during February and March 2004. Figure 5 shows the factor of safety for the control plot during the period of monitoring (September 2003 through late April 2004), while Figure 6 shows the profile changes associated with each period of toe erosion and each bank failure event. Table 4 summarizes the flow and bank conditions at the time of the predicted failures. As is typical, simulated bank failure occurred during periods of bank steepening by hydraulic scour and prolonged periods of bank wetting.

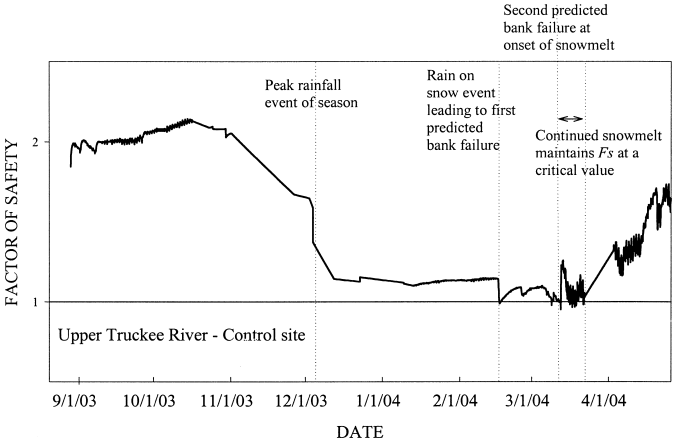

Figure 5. Factor of Safety for Control Site on the Upper Truckee River, California, From September 2003 to Late April 2004.

In the case of the first failure, (February 17, 2004), toe erosion throughout the winter months had contributed to undercutting at the base of the bank. The toe erosion algorithm predicted approximately 0.72 m2 of erosion from the control bank profile before the first predicted failure. In addition, a rain-on-snow event on February 17, 2004, led to reductions in matric suction in all layers and the production of positive pore-water pressures in the third layer of the bank. The combination of changing bank geometry and the reduction of matric suction in the bank thus led to a sufficient reduction in shear strength for the F_S to fall below 1.0.

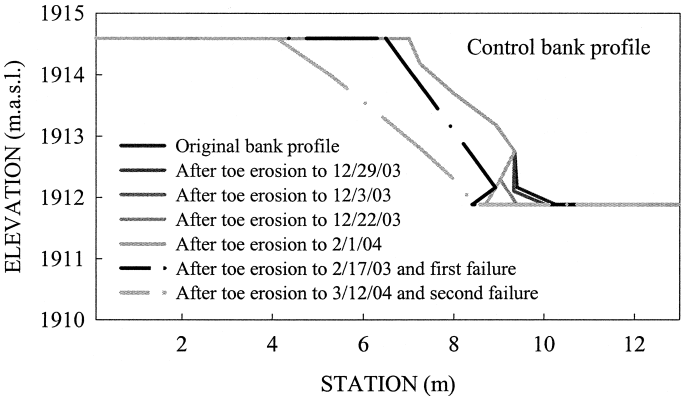

Figure 6. Bank Profile Changes During the Modeling of Toe Erosion and Bank Erosion at the Control Site on the Upper Truckee River, California.

In the case of the second predicted bank failure (March 9, 2004), snowmelt caused the bank to become saturated, and positive pore water pressures again developed in the third layer of the streambank. Failure occurred as a result of a reduction in shear strength related to saturation and a slight lowering of the river's stage causing the loss of confining forces along the bank face. Oversteepening was less a factor in this second failure because the bank angle was flatter as a result of the first failure, and only 0.10 m^2 of toe erosion was predicted to have occurred since that first failure.

The conditions for the third failure stem from further saturation during snowmelt that continued during early March 2004, producing a period of instability from March 12 until March 16, 2004. The additional snowmelt during this time caused both of the top layers in the bank to be almost saturated, and again pore water pressures in the third layer were positive, leading to instability.

Overall, the modeled FS for the control plot was low from mid-December to mid-March, when the tensiometer data showed that the bank started to dry out slightly. The bank stayed wet all winter because of basal snowmelt, and the modeling results showed periodic snowmelt and rain-on-snow events triggered instability in February and March, when river stage

TABLE 4. Critical Conditions at Times of Predicted Bank Failure of the Control Plot.

Predicted Bank Failure Dates	Bank Height (m)	Average Bank Angle at Failure (degrees)	Matric Suction (kPa)			River Stage (m.a.s.l)	Rainfall or Snowmelt?	Toe Erosion From Cross Section (m^2)
			30 cm	100 cm	150 cm			
February 17, 2004	2.7	51.5	1.19	1.85	-1.13	1,913.13	Rain on snow	0.718
March 9, 2004	2.7	45.0	1.92	0.62	-0.51	1,912.96	Snowmelt	0.101
March 12, 2004	2.7	35.0	0.15	0.21	-1.41	1,913.20	Snowmelt	Negligible

was still relatively low. During the time of peak snowmelt later in the spring, the corresponding increase in stage provided confining forces that supported the bank. Saturated banks were therefore more stable during late March and April despite the increased pore-water pressures during this period.

Hydrologic Effects of Vegetation on F_s

The effects of modified cohesion due to matric suction resulted in differences in bank stability relative to the control plot. Bank stability model runs for the vegetated plots are shown in Figures 7 and 8. During autumn, enhanced matric suction at 100 cm resulted in higher F_S values for the vegetated plots compared to the control (Figure 7a). However, this effect declined rapidly after the onset of snowfall in December 2003 as basal melting of temporary snowpacks occurred. The first failure predicted at the pine plot occurred on the same date as that of the first failure at the control plot (February 17, 2004). A second period of instability was also predicted for the pine plot during mid-March 2003 (Figure 7a), showing similar timing of failures as in the control plot. However, in the pine plot, F_S was seen to increase more rapidly in the spring compared to the control plot, coinciding with increased evapotranspiration during early spring. The length of the period of instability thus seems to be reduced in the pine plot, although failures were still predicted to occur.

In the case of the willows, F_S remained greater than 1.0 at all times during the monitoring period, although during some periods stability was in the conditionally stable range (1.01 to 1.3). As no failures were predicted for the Lemmon's willow plot, the only changes to bank geometry throughout the model runs came from erosion at the bank toe. The bank profile in the willow runs thus remained steeper than those of the control and pine runs, which explains why the F_S for the willow plot remains so low during late spring compared to the other two treatments; the drying out trend reflected in the F_S of the pine and control plots had less effect on the willow plot because of the steeper bank angle.

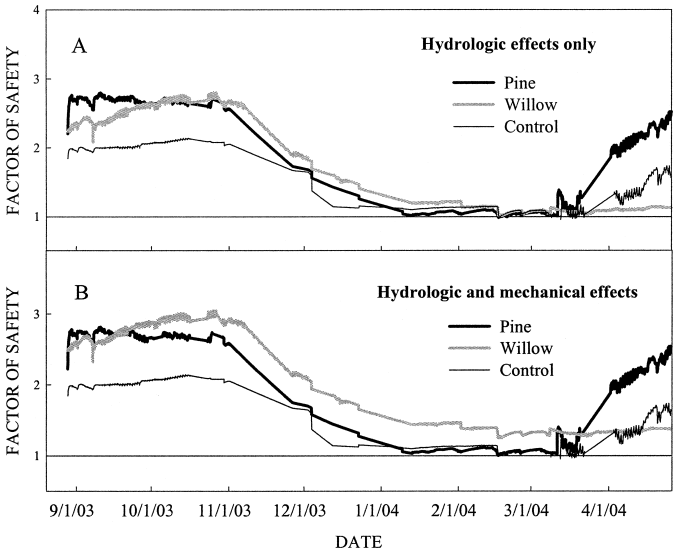

Figure 7. Impact on the Factor of Safety by: (A) Hydrologic Effects Only and (B) Hydrologic and Mechanical Effects of Vegetation at the Upper Truckee River Sites, California.

Combined Mechanical and Hydrologic Effects of Vegetation on F_S

To evaluate the combined mechanical and hydrologic effects of the two species on bank stability, model runs were repeated using the cohesion values as altered by changes in matric suction and due to root reinforcement. Results, expressed by the F_S, are shown in Figures 7 and 8. The small contribution to soil strength from root reinforcement by the lodgepole pines (0.5 kPa) had little effect on F_S throughout the modeling period (Figure 8a), and greatest instability and failures were still predicted for mid-March. In contrast, the cohesion added by the root network of Lemmon's willow (5.5 kPa) had a considerable effect on F_S (Figure 8b), most importantly during the critical wet period during February and March. With the

additional strength provided from enhanced matric suction at the Lemmon's willow site, no bank failures were predicted. In some cases, however, stability was in the conditionally stable range (1.0 to 1.3). With the addition of the mechanical root reinforcement of willows, bank stability was further increased.

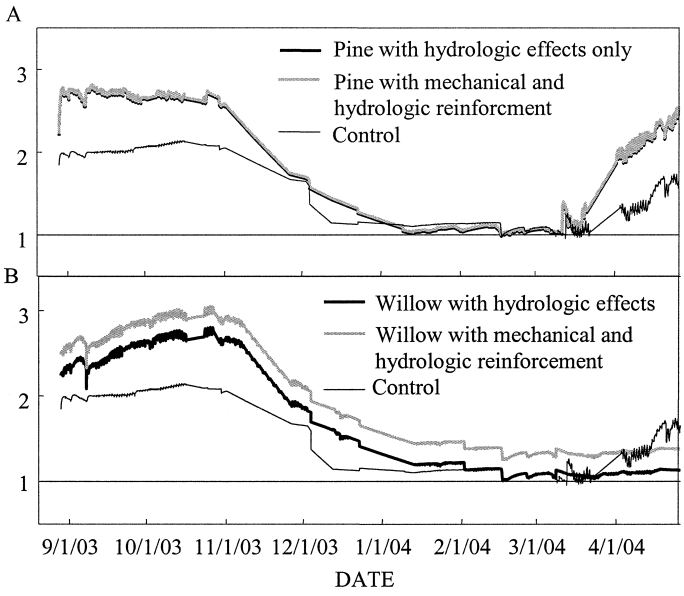

Figure 8. Hydrologic and Mechanical Effects for Pine (A) and Willow (B) at the Upper Truckee Sites, California.

CRITICAL CONDITIONS FOR BANK FAILURE WITH AND WITHOUT VEGETATION

To illustrate the role of riparian vegetation on increasing bank stability, model runs were carried out for a range of bank angles initially using the geotechnical parameters and 2.7 m bank height for the control site. Critical conditions, defined by F_S = 1.0, were calculated and plotted for varying levels of flow and the phreatic surface. Model runs were then repeated using the additional 5.5 kPa of root reinforcement provided by Lemmon's willow and plotted on the same graph (Figure 9). Data for Lemmon's willow were used because of the significant amount of ΔS provided by this species and its potential for use as a bank stabilization measure. Differences in the plotted position of the line of critical conditions for each bank angle, with and without vegetation, represent the effect Lemmon's willow on critical conditions.

Modeling results show that the addition of 5.5 kPa of root reinforcement has a significant effect on the flow depths and water table heights that delimit stable and unstable conditions for each bank angle. The results can be viewed in two ways: (1) the reduction in the angle of an unvegetated bank that would be required to achieve the stability of a vegetated bank of the same angle, and (2) the level of the phreatic surface (degree of saturation) that can be withstood by a vegetated and unvegetated bank of the same angle.

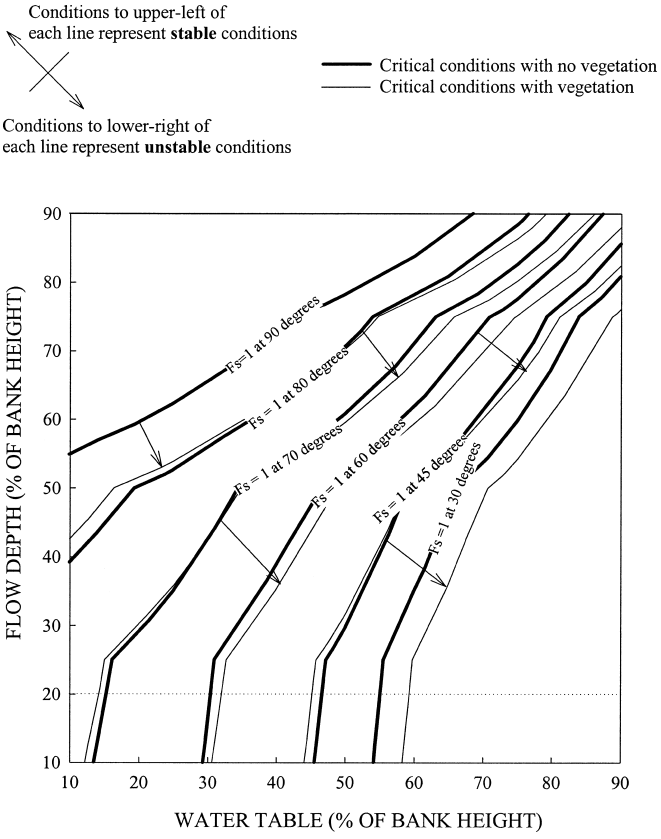

Figure 9. Critical Bank Stability Conditions for the Control Site on the Upper Truckee River, California, With and Without Vegetation for a Range of Bank Angles, Flow Depths, and Phreatic Surface Elevations. Dotted, horizontal line represents a typical low flow depth. Arrows indicate the stabilizing effect of additional bank cohesion (5.5 kPa) from vegetation to a bank of a particular angle.

The addition of vegetation has the same effect as reducing the angle of the bank face, with this effect becoming more significant as the bank angle becomes flatter. Therefore, a vegetated bank with an angle of 90 degrees has similar critical conditions to an unvegetated bank with an angle of 80 degrees. At the other end of the spectrum, a 45-degree vegetated bank has similar critical conditions to an unvegetated bank of less than 30 degrees. Adding 5.5 kPa of root reinforcement to the bank, therefore, has the equivalent effect of reducing the bank angle from 10 degrees to more than 15 degrees depending on the initial angle of the bank. In terms of bank stabilization measures, the

addition of vegetation is equivalent to physically reducing the angle of the bank.

The dotted, horizontal line on Figure 9 represents a typical low flow depth (20 percent of the bank height) at the control site. This depth was chosen because during saturated bank conditions, bank stability can be critical at low flow because of the lack of a confining force to support the bank. As an example, it can be seen that with vegetation a 70-degree bank can withstand an increase in the elevation of the phreatic surface from 15 percent to 33 percent of the bank height. At shallower bank angles, the difference in critical phreatic surface heights between vegetated and unvegetated banks were lower, but even at 45 degrees there was a difference in critical water table depth of 10 percent of the bank height. The effect of the additional strength provided by root reinforcement is therefore equivalent to providing bank drainage (phreatic surface lowering) of as much as 0.5 m.

Comparison of Simulated Failures to Observed Failures

Two failures at the tensiometer sites were noted in the monitoring period during prolonged snowmelt; one was at the control site and the other at the pine site (Table 4). The failure at the pine site occurred on March 12, 2004, one of the dates of failure predicted by the modeling results for this site. The failure noted at the control site actually happened in early April toward the end of a prolonged period of snowmelt. Modeling results did not predict any failures at this site this late in the spring because earlier predicted failures resulted in flatter bank slopes. The F_S for the pine and control sites were found to be very similar throughout this period of maximum instability, but observations from the sites suggest that bank failure actually occurred earlier in the season at the lodgepole pine site compared to the control site. One reason for this may be the concentration of water at certain locations in the bank profile caused by preferential flow along the pine root networks. The higher number of larger diameter roots and the root architecture centered around a main taproot may have caused the pine root networks to be more likely to adversely affect bank hydrology than the willows. As noted above, the willows had a denser and more uniformly distributed root network, both laterally and vertically through the soil profile, with many small roots that created fewer major pathways for preferential flow in the soil.

SUMMARY AND CONCLUSIONS

This study combined the use of field data with numerical simulations using the Bank Stability and Toe Erosion Model (Simon *et al.,* 1999) to identify the critical conditions and controlling factors for bank stability along an unstable reach of the Upper Truckee River, California. Bank failures occur during winter and spring months, brought on by repeated basal melting of snowpacks and rain-on-snow events that maintain saturated conditions for extended periods. Field studies of lodgepole pine and Lemmon's willow were used to quantify the mechanical, hydrologic, and net effects of riparian vegetation on streambank stability. Although results of tensile strength testing showed that roots of both species had similar strength characteristics over the range of root diameters, the greater number and larger root areas for Lemmon's willow provided an order of magnitude more strength (5.5 kPa) than the lodgepole pines (0.5 kPa). The hydrologic effects of the species tested were variable spatially (vertically) and temporally. In the upper 30 cm, vegetated banks were wetter than the control during snowmelt because root networks provided greater opportunities for preferential flow. At 1.0 m depth, about 9 kPa of matric suction developed during summer and autumn from evapotranspiration and extended through early winter, providing 2 to 3 kPa of additional strength. This decreased to less than 1.0 kPa during spring, but the decrease was short-lived as evapotranspiration began anew, resulting in increased matric suction and a much shorter period of critical bank conditions than for the control site.

Lemmon's willow provides a significant increase in bank strength to streambanks along the Upper Truckee River. Model runs that were conducted with the hydrologic and mechanical effects of Lemmon's willow showed no failures during the simulation period. Analysis of critical bank conditions with and without the effects of this species shows that in the presence of Lemmon's willow, banks can withstand steeper slopes (by 10 to 15 degrees) and more saturated conditions. These effects can be considered numerically equivalent to stabilization measures, specifically flattening the bank by grading and/or by providing up to 0.5 m of drainage. The increased stability provided by riparian vegetation indicates that the frequency of bank failures and delivery of fine-grained sediment along the Washoe Meadows reach of the Upper Truckee River could be reduced.

ACKNOWLEDGMENTS

The authors would like to thank the following people and institutions for their help in conducting this study: Phillip Brozek, U.S. Army Corps of Engineers, Sacramento District, and John Reuter, University of California, Davis, Tahoe Research Group, for providing funding for this study; Cyndi Walck, California State Parks, for arranging access to field sites and for providing surveyed cross sections of the Upper Truckee River; Brian Bell, USDA-ARS National Sedimentation Laboratory, and Lauren Farrugia, University of Mississippi, for installing the digital instruments; Dave Roberts, Lahontan Regional Water Quality Control Board, for maintaining the digital instruments during the period of study; and Lyndsey Percival, University of Nottingham, for help in collecting root strength and distribution data.

LITERATURE CITED

Abernethy, B., 1999. On the Role of Woody Vegetation in Riverbank Stability. PhD Thesis, Monash University, Melbourne, Australia.

Bishop, A.W. 1955. The Use of the Slip Circle in the Stability Analysis of Slopes. Geotechnique 5:7-17.

Bohm, W., 1979. Methods of Studying Root Systems. Springer-Verlag, Berlin, Germany.

Carson, M.A. and Kirkby, M. J., 1972. Hillslope Form and Process. Cambridge University Press, Cambridge, England, 475 pp.

Dingman, S.L., 2001. Physical Hydrology (Second Edition). Prentice Hall, Upper Saddle River, New Jersey.

Durocher, M.G., 1990. Monitoring Spatial Variability in Forest Interception. Hydrological Processes 4:215-229.

Fredlund, D.G., N.R. Morgenstern, and R.A. Widger, 1978. The Shear Strength of Unsaturated Soils. Canadian Geotechnical Journal 15:313-321.

Fredlund, D.G. and H. Rahardjo, 1993. Soil Mechanics of Unsaturated Soils. John Wiley and Sons, New York, New York.

Glancy, P.A., 1988. Streamflow, Sediment Transport, and Nutrient Transport at Incline Village, Lake Tahoe, Nevada 1970-1973. U.S. Geological Survey Water Supply Paper 2313, U.S. Government Printing Office, Washington, D.C. 53 pp.

Gray, D.H. and R.B. Sotir, 1996. Biotechnical and Soil Bioengineering Slope Stabilization: A Practical Guide for Erosion Control. John Wiley and Sons Inc, New York, New York.

Greenway, D.R., 1987. Vegetation and Slope Stability. *In:* Slope Stability, M.G. Anderson and K.S. Richards (Editors). John Wiley and Sons Ltd, New York, New York, pp. 187-230.

Hanson, G.J., 1990. Surface Erodibility of Earthen Channels at High Stresses: Part II. Developing an *In-Situ* Testing Device. Transactions of the ASAE 33(1):132-137.

Hanson, G.J., 1991. Development of a Jet Index to Characterize Erosion Resistance of Soils in Earthen Spillways. Transactions of the ASAE 34(5):2015-2020.

Hanson, G.J. and A. Simon, 2001. Erodibility of Cohesive Streambeds in the Loess Area of the Midwestern USA. Hydrological Processes 15(1):23-38.

Hill, B.R. and K.M. Nolan, 1990. Suspended Sediment Factors, Lake Tahoe Basin, California-Nevada. *In:* International Mountain Watershed Symposium, 1988 Proceedings, South Lake Tahoe, California, I.G. Poppoff, C.R. Goldman, S.L. Loeb, and L.B. Leopold (Editors). Tahoe Resource Conservation District, South Lake Tahoe, California, pp. 179-189.

Jassby, A.D., C.R. Goldman, J.E. Reuter and R.C. Richards, 1999. Origins and Scale Dependence of Temporal Variability in the Transparency of Lake Tahoe, California-Nevada. Limnol. Oceanogr. 44(2):282-294.

Jassby, A.D., J.E. Reuter, and C.R. Goldman, 2003. Determining Long-Term Water Quality Change in the Presence of Climatic Variability: Lake Tahoe (USA). Can. J. Fish. Aquat. Sci. 60:1452-1461.

Kroll, C.G., 1976. Sediment Discharge From Highway Cut-Slopes in the Lake Tahoe Basin, California. U.S. Geological Survey Water Resources Investigations Report 76-19.

Langendoen, E.J., 2000. CONCEPTS – Conservational Channel Evolution and Pollutant Transport System Software Manual. USDA-ARS National Sedimentation Laboratory Research Report 16, Oxford, Mississippi.

Little, W.C., C.R. Thorne, and J.B. Murphy, 1982. Mass Bank Failure Analysis of Selected Yazoo Basin Streams. Transcripts of the American Society of Agricultural Engineering 25:1321-1328.

Lohnes, R.A. and R.L. Handy, 1968. Slope Angles in Friable Loess. Journal of Geology 76(3):247-258.

Lutenegger, J.A. and B.R. Hallberg, 1981. Borehole Shear Test in Geotechnical Investigations. ASTM Special Publications 740, pp. 566-578.

Nolan, K.M. and B.R. Hill, 1991. Suspended Sediment Budgets for Four Drainage Basins Tributary to Lake Tahoe, California and Nevada. U.S. Geological Survey Water-Resources Investigations Report 91-4054, Sacramento, California, 40 pp.

Pollen, N., 2004. The Effects of Riparian Vegetation on Streambank Stability: Mechanical and Hydrological Interactions. Ph.D. Thesis, University of London, United Kingdom, 320 pp.

Pollen, N., A. Simon, and A.J.C. Collison, 2004. Advances in Assessing the Mechanical and Hydrologic Effects of Riparian Vegetation on Streambank Stability. *In:* Riparian Vegetation and Fluvial Geomorphology, S. Bennett and A. Simon (Editors). Water Science and Applications, AGU 8:125-139.

Reuter, J.E. and W.W. Miller, 2000. Aquatic Resources, Water Quality, and Limnology of Lake Tahoe and Its Upland Watershed. *In:* Lake Tahoe Watershed Assessment, D.D. Murphy and C.M. Knopp (Editors). General Technical Report PSW-GTR-175, U.S. Department of Agriculture-Forest Service, Pacific Southwest Research Station. Albany, California, Vol. 1, Chapter 4, pp. 215-399.

Rowe, T.G., D.K. Saleh, S.A. Watkins, and C.R. Kratzer, 2002. Streamflow and Water-Quality Data for Selected Watersheds in the Lake Tahoe Basin, California and Nevada, Through September 1998. U.S. Geological Survey Water Resources Investigations Report 02-4030, Carson City, Nevada, 117 pp.

Selby, M.J., 1993. Hillslope Materials and Processes. Oxford University Press, Oxford, United Kingdom.

Simon, A. and J. Castro, 2003. Measurement and Analysis of Alluvial Channel Form. *In:* Tools in Fluvial Geomorphology, M. Kondolf and H. Piegay (Editors). John Wiley and Sons, New York, New York, pp. 291-322.

Simon, A. and A.J.C. Collison, 2002. Quantifying the Mechanical and Hydrologic Effects of Riparian Vegetation on Stream-Bank Stability. Earth Surface Processes and Landforms 27(5):527-546.

Simon, A., A. Curini, S. Darby, and E. Langendoen, 1999. Stream-Bank Mechanics and the Role of Bank and Near-Bank Processes in Incised Channels. *In:* Incised River Channels, S. Darby and A. Simon (Editors). John Wiley and Sons, New York, New York, pp. 123-152.

Simon, A., A. Curini, S.E. Darby, and E.J. Langendoen, 2000. Bank and Near-Bank Processes in an Incised Channel. Geomorphology 35:193-217.

Simon, A., E. Langendoen, R. Bingner, R. Wells, A. Heins, N. Jokay, and I. Jaramillo, 2003. Lake Tahoe Basin Framework Implementation Study: Sediment Loadings and Channel Erosion. National Sedimentation Laboratory Technical Report 39, USDA-ARS National Sedimentation Laboratory, Oxford, Mississippi, 320 pp.

Simon, A., W.J. Wolfe, and A. Molinas, 1991. Mass Wasting Algorithms in an Alluvial Channel Model. *In:* Proceedings of the 5th Federal Interagency Sedimentation Conference. U.S. Subcommittee on Sedimentation, Vol. 2, pp. 8-22 to 8-29, CD-ROM.

Stokes, A. and C. Mattheck, 1996. Variation of Wood Strength in Tree Roots. Journal of Experimental Botany 47(298):693-699.

Stubblefield, A.P., 2002. Spatial and Temporal Dynamics of Watershed Sediment Delivery, Lake Tahoe, California. PhD Dissertation. University of California at Davis, Davis, California.

Thorne, C.R., 1982. Processes and Mechanisms of River Bank Erosion. *In:* Gravel-Bed Rivers, R.D. Hey, J.C. Bathurst, and C.R. Thorne (Editors). John Wiley and Sons, Chichester, England, pp. 227-271.

Thorne, C.R., 1990. Effects of Vegetation on Riverbank Erosion and Stability. *In:* Vegetation and Erosion, J.B. Thornes (Editor). John Wiley and Sons Inc, Chichester, England, pp. 125-143.

Thorne, C.R., J.B. Murphey, and W.C. Little, 1981. Appendix D: Bank Stability and Bank Material Properties in the Bluffline Streams of North-West Mississippi. U.S. Department of Agriculture, Agricultural Research Service, National Sedimentation Laboratory, Oxford, Mississippi.

Waldron, L.J., 1977. The Shear Resistance of Root-Permeated Homogeneous and Stratified Soil, J. Soil Science Soc. Amer. 41:843-849.

Wu, T.H., W.P. McKinnell III, and D.N. Swanston, 1979. Strength of Tree Roots and Landslides on Prince of Wales Island, Alaska. Canadian Geotechnical Journal 16:19-33.